Chapter 2
Theory of Optomechanics

Abstract In this chapter, we describe the basic aspects of optical cavities, mechanical resonators, and cavity optomechanical systems, e.g. optical response of the cavity, mechanical dissipation (thermal decoherence), dilution technique, the (double) optical spring, quantum back-action, phase-induce back-action noise, and Raman decoherence. Especially, the dilution technique due to the gravitational and optical potential is explained in detail, because it is one of the most important technical features in our experiment. This chapter also presents the basic concepts and mathematical tools for understanding later chapters.

Keywords Gravitaional dilution · Optical dilution · Cavity optomechanics · Quantum back-action · Bad cavity condition

2.1 Optical System

There are two equally important aspects in the physical theory: the mathematical formalism of the theory, and its intuitive interpretation. In this section, we describe the mathematical formalism for the quantization of light and the result. Also, we present intuitive interpretations of classical/quantum fluctuation, which is so-called the *ball-on-stick* picture.

2.1.1 The Quantized Electromagnetic Field

In 1927, Paul Dirac proposed quantization of the electromagnetic field in order to solve the problem of the wave-particle duality. In this quantum theory, each mode of a radiation field is identified by a quantized simple harmonic oscillator.f The properties of the quantized field are introduced in the context of an optical cavity mode with angular frequency of $\omega_{\boldsymbol{k}}$. The positive and negative components of the electric field can be written in terms of the boson creation and annihilation operators, $\hat{a}_{\boldsymbol{k}}^{\dagger}$ and $\hat{a}_{\boldsymbol{k}}$, and the spatial mode function, $\boldsymbol{u}(\boldsymbol{r})$:

N. Matsumoto, *Classical Pendulum Feels Quantum Back-Action*,
Springer Theses, DOI 10.1007/978-4-431-55882-8_2

$$\boldsymbol{E}^{(+)}(\boldsymbol{r},t) = i\sum_{\boldsymbol{k}}\left(\frac{\hbar\omega_{\boldsymbol{k}}}{2\varepsilon_0}\right)^{1/2}\hat{a}_{\boldsymbol{k}}\boldsymbol{u}(\boldsymbol{r})\exp(-i\omega_{\boldsymbol{k}}t), \tag{2.1}$$

$$\boldsymbol{E}^{(-)}(\boldsymbol{r},t) = -i\sum_{\boldsymbol{k}}\left(\frac{\hbar\omega_{\boldsymbol{k}}}{2\varepsilon_0}\right)^{1/2}\hat{a}^{\dagger}_{\boldsymbol{k}}\boldsymbol{u}(\boldsymbol{r})^{*}\exp(i\omega_{\boldsymbol{k}}t). \tag{2.2}$$

Here, $\hbar$ is the Dirac constant and ε_0 is the permittivity of free space. The sum of the positive and negative components gives the whole electric field given by

$$\boldsymbol{E}(t) = i\sum_{\boldsymbol{k}}\left(\frac{\hbar\omega_{\boldsymbol{k}}}{2\varepsilon_0}\right)^{1/2}\left[\hat{a}_{\boldsymbol{k}}\boldsymbol{u}(\boldsymbol{r})\exp(-i\omega_{\boldsymbol{k}}t) - \hat{a}^{\dagger}_{\boldsymbol{k}}\boldsymbol{u}(\boldsymbol{r})^{*}\exp(i\omega_{\boldsymbol{k}}t)\right]. \tag{2.3}$$

The creation and annihilation operators are dimensionless, and satisfy the boson commutation relations,

$$[\hat{a}_{\boldsymbol{k}},\hat{a}_{\boldsymbol{k}'}] = [\hat{a}^{\dagger}_{\boldsymbol{k}},\hat{a}^{\dagger}_{\boldsymbol{k}'}] = 0,\ [\hat{a}_{\boldsymbol{k}},\hat{a}^{\dagger}_{\boldsymbol{k}'}] = \delta_{\boldsymbol{k}\boldsymbol{k}'}. \tag{2.4}$$

These commutation relations can allow us to distinct between classical and quantum optics. In classical optics, an equivalent of Eq. (2.3) can be found by replacing the annihilation and creation operators with complex field amplitudes. The amplitudes in classical optics commute, and thus they are not limited by the Heisenberg uncertainty relation and its consequences. In quantum mechanics, however, the operators must be Hermitian in order to represent observable quantities. The annihilation and creation operators are not Hermitian, and are thus not observables. They can be written in terms of a Hermitian operator pair for the amplitude quadrature, $\hat{X}_1$, and the phase quadrature, $\hat{X}_2$:

$$\hat{a} = \frac{1}{2}(\hat{X}_1 + i\hat{X}_2), \tag{2.5}$$

$$\hat{a}^{\dagger} = \frac{1}{2}(\hat{X}_1 - i\hat{X}_2), \tag{2.6}$$

The quadrature operators for the amplitude and phase are:

$$\hat{X}_1 = \hat{a} + \hat{a}^{\dagger}, \tag{2.7}$$

$$\hat{X}_2 = -i(\hat{a} - \hat{a}^{\dagger}). \tag{2.8}$$

The amplitude and phase quadratures represent non-commuting observable parameters. The operator for an arbitrary quadrature, ξ, can be defined using a linear combination of $\hat{X}_1$ and $\hat{X}_2$,

$$\hat{X}_{\xi} = \hat{X}_1\cos(\xi) + \hat{X}_2\sin(\xi). \tag{2.9}$$

2.1.2 The Heisenberg Uncertainty Principle

The Heisenberg uncertainty principle (HUP) [1] quantifies the ultimate precision of continuous measurement of non-commuting observable parameters, as described in Chap. 1. HUP tells us that if any two observable parameters, $\hat{O}_1$ and $\hat{O}_2$, satisfy the commutation relation,

$$[\hat{O}_1, \hat{O}_2] = \xi, \tag{2.10}$$

they are bounded by HUP,

$$\Delta\hat{O}_1 \Delta\hat{O}_2 \geq \frac{|\xi|}{2}, \tag{2.11}$$

where $\Delta\hat{O}$ is the standard deviation of the operator $\hat{O}$. The standard deviation is defined by

$$\Delta\hat{O} = \sqrt{\langle\hat{O}^2\rangle - \langle\hat{O}\rangle^2}. \tag{2.12}$$

The variance of the operator is the square of the standard deviation,

$$V = (\Delta\hat{O})^2. \tag{2.13}$$

The commutator relation of the amplitude and the phase quadratures of the electromagnetic field is

$$[\hat{X}_1, \hat{X}_2] = 2i, \tag{2.14}$$

and thus HUP is

$$\Delta\hat{X}_1 \Delta\hat{X}_2 \geq 1. \tag{2.15}$$

This relation shows that the trade-off between the fluctuation of the amplitude quadrature and that of the phase quadrature. Therefore, this also shows the trade-off between the shot noise and the radiation pressure shot noise for the force measurement.

2.1.3 States of Light

Here, several common states (a coherent state, a vacuum state, a squeezed state of light, and a classically noisy state) are described and shown in *ball-on-stick* pictures. In the ball-on-stick pictures, the classical steady-state coherent amplitude of the field is represented as a stick, while the fluctuation of light is represented as a ball on the

stick, which is analogous to the phasor diagram used in classical physics where the orthogonal axes are the real and imaginary parts of an electromagnetic field. Various states of light can be visually understood by this.

- **The coherent state**
  A coherent state is a minimum-uncertainty state with equal uncertainties in the two quadrature components, so that

$$\Delta\hat{X}_1 = \Delta\hat{X}_2 = 1. \tag{2.16}$$

  The quadrature fluctuations of the coherent state have no frequency dependence, and obey Poissonian statistics. For the coherent state, the sidebands are randomly distributed in phase, and thus there is no special phase. Although the coherent state is realized by the laser, the laser light has excess noise below the MHz region, whereas we measured a pendulum motion. Thus, stabilization of the laser intensity fluctuation is necessary for measurement of the quantum back-action. In our case, the quantum back-action was now estimated by measurement of the classical behaver, see also in Fig. 6.5a.
- **The vacuum state**
  A vacuum state is also a minimum-uncertainty state with equal uncertainties in the two quadrature components, but it has no coherent amplitude ($\bar{a} = \langle\hat{a}(t)\rangle = 0$). It always occupies all frequency, spatial, and polarization modes. The vacuum state is important in quantum-optical experiments, since it enters optical systems in any unfilled ports of the beam splitters, cavities, and partially transmissive mirrors. In our case, the vacuum state prevents stabilization of the laser intensity noise from achieving the minimum uncertainty level, see in Sect. 5.1 and Appendix.
- **The squeezed state**
  A squeezed state is a non-classical state in which fluctuation is reduced below the symmetric quantum limit in one quadrature component. In order to satisfy HUP, the standard deviation of the orthogonal quadrature must be greater than the quantum noise limit and the product of the two quadratures greater than or equal to unity. If the amplitude quadrature is reduced, it is called the amplitude squeezed state, and vice versa. Thus, the minimum uncertainty amplitude squeezed state, for example, has

$$\Delta\hat{X}_1 = 1/z, \tag{2.17}$$

$$\Delta\hat{X}_2 = z, \tag{2.18}$$

  where z is a real and a positive number. The amplitude-squeezed state is shown in Fig. 2.1.
- **Classically noisy states**
  In general, lasers produce non-minimum-uncertainty states, which have excess noise of classical origin at sideband frequencies below the MHz region. The classical noise of a laser is often many times greater than the quantum noise in both quadratures,

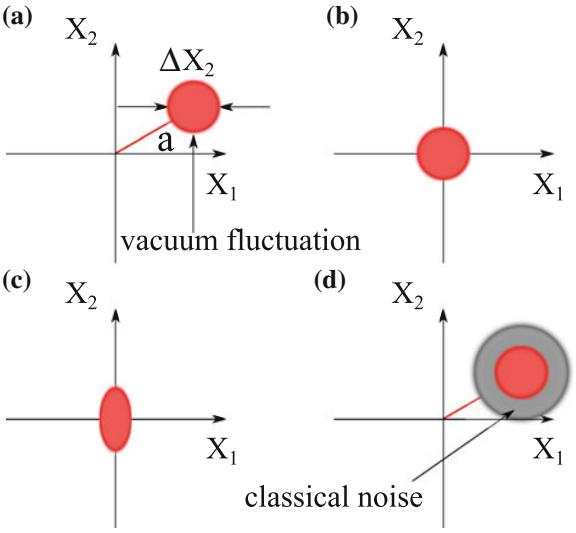

Fig. 2.1 Ball-and-stick pictures for states of light. **a** Coherent state is represented. **b** Vacuum state is represented. **c** Amplitude squeezed state is represented. **d** Classically noisy state is represented

$$\Delta\hat{X}_1 \geq 1, \ \Delta\hat{X}_2 \geq 1. \tag{2.19}$$

The classical noise can be reduced via: passive noise suppression using an optical cavity [2]; active feedback control ; or both. The noisy state is characterized by comparing with the shot noise level in units of dB (so-called the relative to the shot-noise level) and its coherent laser power in units of $1/\mathrm{Hz}^{1/2}$ (so-called relative intensity noise). The former is an useful index for quantum measurements, such as observation of the quantum back-action and generation of the squeezed state. The latter is an useful index for force measurement, such as that used in gravitational-wave detectors.

2.1.4 Optical Cavity

Fabry-Perot interferometers, often referred to as (optical) cavities, consist of two or more partially transmissive mirrors in order to make the light resonate inside it. In this section, the equation of motion for a cavity mode is introduced; we then obtain the reflected and transmitted fields using this equation.

2.1.4.1 Equation of Motion

Consider the empty cavity shown in Fig. 2.2. It is made of three partially transmissive optics labeled, in, out, and l, referring to the input coupler, the output coupler, and

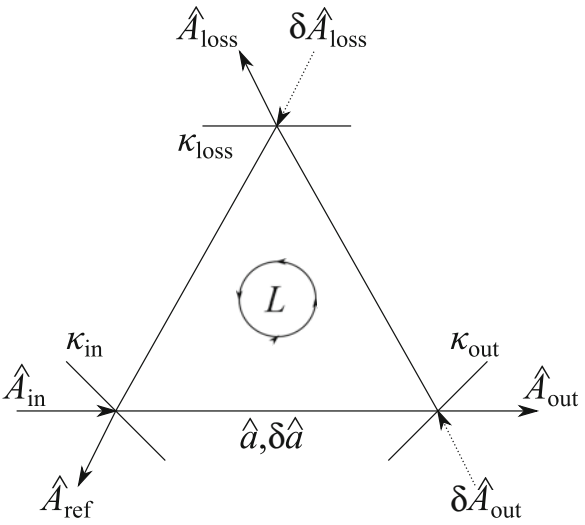

Fig. 2.2 Layout of the optical cavity. Consider a cavity composed of two mirrors: an input coupler, with a decay rate of κ_{in}; an output coupler, with a decay rate of κ_{out}; a mirror to represent intracavity loss, with a decay rate of κ_{loss}; and the roundtrip length of the cavity, L. The cavity mode is labeled $\hat{a}$. The extracavity fields are: $\hat{A}_{\text{in}}$, $\hat{A}_{\text{out}}$, $\hat{A}_{\text{ref}}$, $\hat{A}_{\text{loss}}$, $\delta\hat{A}_{\text{out}}$ and $\delta\hat{A}_{\text{loss}}$

the partially transmissive mirror used to simulate losses, respectively. The equation of motion for cavity mode $\hat{a}$ in units of $\sqrt{\text{photon}}$ is [3]

$$\dot{\hat{a}} = -(i\omega_{\text{c}} + \kappa)\hat{a} + \sqrt{2\kappa_{\text{in}}}\hat{A}_{\text{in}}e^{-i\omega_A t} + \sqrt{2\kappa_{\text{out}}}\hat{A}_{\text{out}} + \sqrt{2\kappa_{\text{loss}}}\hat{A}_{\text{loss}}, \tag{2.20}$$

where the driving field, A_{in}, in units of $\sqrt{\text{photon}/\text{s}}$ has a coherent amplitude at frequency ω_{A}; the other fields, A_{out} and A_{loss}, are assumed to be in the vacuum state. The cavity mode has a resonant frequency of ω_c.

The equation of motion can be written in the rotating frame of reference by setting

$$\hat{a} \rightarrow \hat{a}e^{-i\omega_A t}, \tag{2.21}$$

$$\hat{A}_{\text{in}} \rightarrow \hat{A}_{\text{in}}e^{-i\omega_A t}, \tag{2.22}$$

and thus

$$\dot{\hat{a}} = (i\triangle - \kappa)\hat{a} + \sqrt{2\kappa_{\text{in}}}\hat{A}_{\text{in}} + \sqrt{2\kappa_{\text{out}}}\hat{A}_{\text{out}} + \sqrt{2\kappa_{\text{loss}}}\hat{A}_{\text{loss}}, \tag{2.23}$$

where $\Delta = \omega_A - \omega_c$ is the cavity detuning [i.e., the positive (negative) detuning means the blue-detuning (red-detuning)]. In the mean-field approximation [4, 5], the amplitude decay rates for each mirror are given by the amplitude transmissivity divided by the round trip time, $\tau = L/c$, where L is the roundtrip of the cavity. That is,

$$\kappa_{\text{in}} = \frac{\sqrt{T_{\text{in}}}}{\tau} \simeq \frac{T_{\text{j}}}{2\tau}$$
$$\kappa_{\text{out}} \simeq \frac{T_{\text{out}}}{2\tau}$$
$$\kappa_{\text{loss}} \simeq \frac{1 - \mathscr{L}_c}{2\tau}, \tag{2.24}$$

where $\mathscr{L}_{\text{c}}$ is the cavity round-trip loss. The total decay rate is given by

$$\kappa = \kappa_{\text{in}} + \kappa_{\text{out}} + \kappa_{\text{loss}}. \tag{2.25}$$

In the steady state, the cavity mode can be found by setting $\dot{\hat{a}} = 0$ and considering the time-independent component $\bar{a}$. Given that the steady state amplitudes of the fields $\bar{A}_{\text{out}} = \bar{A}_{\text{loss}} = 0$, the steady state cavity mode is given by

$$\bar{a} = \frac{\sqrt{2\kappa_{\text{in}}}}{\kappa - i\triangle} \bar{A}_{\text{in}}. \tag{2.26}$$

This equation enables us to obtain the reflected and transmitted fields as a function of detuning in the following was. We are also interested in the Fourier components of the cavity mode. These can be found by Fourier transforms of the operators,

$$Q(\omega) = \int_{-\infty}^{\infty} Q(t) \exp(-i\omega t) dt, \tag{2.27}$$

for $Q = \hat{a}$, $\hat{A}_{\text{in}}$, $\hat{A}_{\text{out}}$, and $\hat{A}_{\text{loss}}$. The equation of motion in the frequency domain is

$$-i\omega\delta\hat{a} = (i\triangle - \kappa)\delta\hat{a} + \sqrt{2\kappa_{\text{in}}}\delta\hat{A}_{\text{in}} + \sqrt{2\kappa_{\text{in}}}\delta\hat{A}_{\text{out}} + \sqrt{2\kappa_{\text{loss}}}\delta\hat{A}_{\text{loss}}, \tag{2.28}$$

where ω is the sideband frequency. Simply put, this fluctuating term induces the quantum back-action force (details are described in Sect. 2.3).

2.1.4.2 Reflected and Transmitted Fields

Using the cavity input-output relations [3], the reflected field, A_{ref} and transmitted field, A_{trans}, can be determined:

$$A_{\text{trans}} = \sqrt{2\kappa_{\text{out}}}a - A_{\text{out}},$$
$$A_{\text{ref}} = \sqrt{2\kappa_{\text{in}}}a - A_{\text{in}}, \tag{2.29}$$

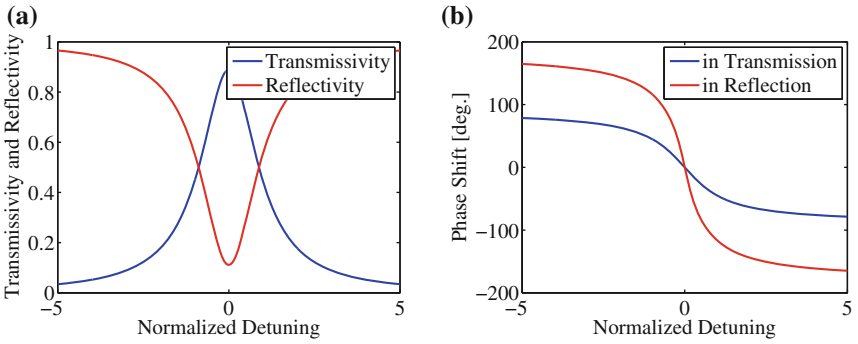

Fig. 2.3 Optical cavity. These show the reflected and transmitted fields as a function of detuning normalized by the cavity decay rate. **a** The (power) reflectivity and transmissivity are shown. **b** The phase shifts in reflection and transmission are shown

which give

$$\bar{A}_{\mathrm{trans}} = \frac{2\sqrt{\kappa_{\mathrm{in}}\kappa_{\mathrm{out}}}}{\kappa - i\triangle}\bar{A}_{\mathrm{in}}, \tag{2.30}$$

$$\bar{A}_{\mathrm{ref}} = \frac{2\kappa_{\mathrm{in}} - \kappa + i\triangle}{\kappa - i\triangle}\bar{A}_{\mathrm{in}}. \tag{2.31}$$

The amplitude transmissivity and reflectivity of the cavity are respectively given by

$$t(\triangle) = \frac{\bar{A}_{\mathrm{trans}}}{\bar{A}_{\mathrm{in}}} = \frac{2\sqrt{\kappa_{\mathrm{in}}\kappa_{\mathrm{out}}}}{\kappa - i\triangle}, \tag{2.32}$$

$$r(\triangle) = \frac{\bar{A}_{\mathrm{ref}}}{\bar{A}_{\mathrm{in}}} = \frac{2\kappa_{\mathrm{in}} - \kappa + i\triangle}{\kappa - i\triangle}, \tag{2.33}$$

and both of them are shown in Fig. 2.3. By using these equations, one can experimentally estimate important parameters, i.e., κ, κ_{in} and κ_{out}, see in Sects. 6.1 and 6.3.

2.2 Mechanical Oscillator

In this section, we describe the mechanical oscillator, especially concerning mechanical dissipation. Mechanical dissipation is one of the most important parameters, because the Fluctuation-Dissipation Theorem (FDT) [6] connects the spectrum of the thermal fluctuating force to the mechanical dissipation in the system, which is given by

$$S^{(2)}_{\mathrm{FF,th}} = \frac{2k_{\mathrm{B}}T_{\mathrm{th}}}{\omega}\mathrm{Im}\chi_{\mathrm{m}} = 4k_{\mathrm{B}}T_{\mathrm{th}}\gamma_{\mathrm{m}}m. \tag{2.34}$$

Here, k_{B} is the Boltzmann constant, T_{th} is the temperature of the thermal bath, χ_{m} is the mechanical susceptibility derived below, ω is the sideband frequency, γ_{m} is the mechanical damping rate (i.e., it represents the dissipation) and m is the mass of the mechanical oscillator. This equation represents that the reduction of the thermal noise requires a low mechanical dissipation and a low bath temperature. To reduce the dissipation, we used gravitational *dilution* technique. Details are described below.

2.2.1 Mechanical Normal Modes

Let us consider a suspended mirror (i.e., pendulum) having a resonant frequency of ω_m, naturally assuming that the mode spectrum is sufficiently sparse such that there is no spectral overlap with other mechanical modes, such as a rocking mode and a violin mode. This condition can be easily satisfied by choosing appropriate parameters [7]. The equation of motion for the position of the mirror, $x(t)$, can be described by

$$m\ddot{x} + 2m\gamma_{\mathrm{m}}\dot{x} + m\omega_{\mathrm{m}}^2 x = F_{\mathrm{ext}}. \tag{2.35}$$

Here, m is the mass of the pendulum, γ_{m} is the amplitude damping rate (i.e., the mechanical quality factor is $Q_{\mathrm{m}} = \omega_{\mathrm{m}}/2\gamma_{\mathrm{m}}$), ω_{m} i the resonant frequency of the oscillator, and $F_{\mathrm{ext}}(t)$ is the external force acting on the mirror. Even if there is no external force, it is given by the thermal fluctuating force.

To solve this equation, we again introduce the Fourier transform via $x(\omega) = \int_{-\infty}^{\infty} dt\, \exp(-i\omega t)x(t)$. Then, the mechanical susceptibility $\chi_{\mathrm{m}}(\omega)$ connecting the external force to the displacement of the oscillator is given by

$$\chi_{\mathrm{m}}(\omega) \equiv \frac{x(\omega)}{F_{\mathrm{ext}}(\omega)} = \frac{1}{m}\frac{1}{\omega_{\mathrm{m}}^2 - \omega^2 + 2i\omega\gamma}. \tag{2.36}$$

The stationary response is given by $\chi_{\mathrm{m}}(0) = (m\omega_{\mathrm{m}}^2)^{-1} = 1/k_{\mathrm{m}}$, where k_{m} is the spring constant.

A quantum-mechanical treatment of the mechanical harmonic oscillator leads to the Hamiltonian

$$\hat{H} = \hbar\omega_{\mathrm{m}}\hat{c}^{\dagger}\hat{c} + \frac{1}{2}\hbar\omega_{\mathrm{m}}. \tag{2.37}$$

Here, the phonon creation, $\hat{c}^\dagger$, and annihilation, $\hat{c}$, operators have been introduced similarly to Eqs. (2.7), (2.8), with

$$\hat{x} = x_{\mathrm{zpf}}(\hat{c} + \hat{c}^\dagger), \tag{2.38}$$

$$\hat{p} = -im\omega_{\mathrm{m}} x_{\mathrm{zpf}}(\hat{c} - \hat{c}^\dagger), \tag{2.39}$$

where

$$x_{\mathrm{zpf}} = \sqrt{\frac{\hbar}{2m\omega_{\mathrm{m}}}} \tag{2.40}$$

is the zero-point fluctuation (root-meas-square) amplitude of the mechanical oscillator. The quantity $\hat{c}^\dagger\hat{c}$ is the phonon number operator, whose average is denoted by $\bar{n} = \langle \hat{c}^\dagger \hat{c} \rangle$. In general, the mechanical oscillator is coupled to a high-temperature bath, and thus the average phonon number will evolve according to the expression [8]

$$\frac{d}{dt}\langle n \rangle = -2\gamma_{\mathrm{m}} \left(\langle n \rangle - \bar{n}_{\mathrm{th}} \right). \tag{2.41}$$

For an oscillator that is initially in the ground state, the time dependence of the occupation is given by

$$\frac{d}{dt}\langle n \rangle_{t=0} = 2\bar{n}_{\mathrm{th}}\gamma_{\mathrm{m}} \simeq \frac{k_{\mathrm{B}} T_{\mathrm{th}}}{\hbar Q_{\mathrm{m}}}, \tag{2.42}$$

where $\bar{n}_{\mathrm{th}}$ is the average phonon number of the thermal bath, T_{th} is the temperature of the thermal bath, and here we suppose the mechanical decay rate γ_{m} has *no* dependence on frequency for the sake of simplicity. Equation (2.42) represents the thermal decoherence rate having the unit of Hz, because it gives the inverse time of the absorption of a phonon from the environment. This expression shows that in order to attain a low thermal decoherence, a high mechanical quality factor, Q_{m}, and a low temperature bath are important. In addition, from this equation, the number of coherent oscillations in the presence of thermal decoherence n_{osc} is given by,

$$n_{\mathrm{osc}} = \omega_{\mathrm{m}} \times \frac{\hbar Q_{\mathrm{m}}}{k_{\mathrm{B}} T_{\mathrm{th}}} = Q_{\mathrm{m}} \cdot f_{\mathrm{m}} \times \frac{h}{k_{\mathrm{B}} T_{\mathrm{th}}}. \tag{2.43}$$

Thus, the "$Q_{\mathrm{m}} \cdot f_{\mathrm{m}}$" product quantifies the decoupling of the mechanical resonator from a thermal environment. Note that full coherence over one mechanical period is obtained for $Q_{\mathrm{m}} \cdot f_{\mathrm{m}} > k_{\mathrm{B}} T_{\mathrm{th}}/\hbar$, i.e., $Q_{\mathrm{m}} \cdot f_{\mathrm{m}} > 6 \times 10^{12}$ Hz is a minimum requirement for room-temperature quantum optomechanics. One might consider that satisfying the criteria is impossible on the macroscopic scale; however, the *dilution* techniques described below will enable us to realize it.

2.2.2 Mechanical Dissipation & Dilution Techniques

The energy loss of mechanical oscillations is quantified by the (amplitude) mechanical dissipation rate, $\gamma_m = \omega_m/2Q_m$. Here, we introduce the loss mechanisms:

- Viscous damping is mainly caused by interactions with the surrounding gas atoms. A resistance force proportional to the velocity is applied to the oscillator, which is given by $\gamma_{gas} = SP\sqrt{m_{mol}}/(2C\sqrt{k_B T m})$, where C is a dimensionless constant of order unity that depends on the shape of the oscillator, S is the cross-sectional area, P the pressure, m_{mol} the mass of a residual molecule of the gas, and m the mass of a mechanical oscillator [9]. In our case, the gas damping will become an issue in future, see in Chap. 7.
- Clamping losses are due to radiation of elastic waves into the substrate through the supports of the oscillator. In our case, a thin tungsten wire is clamped between two aluminum plates at the top, while a mirror is attached to the wire using an epoxy glue at the bottom. Although this lossy configuration has sufficient quality factor for observing the quantum back-action, it will not be sufficient for future experiments. Therefore, we must change it to other relatively lossless materials, such as stainless steels (See Chap. 7).
- A thermoelastic damping is a fundamental anharmonic effect, which is caused by heat flow along the temperature gradients. This effect often causes problems, such as a mirror thermal noise, because the temperature gradients often occur at around the laser beam spot on the mirror. In our case, the mirror thermal noise has been negligible until now; however, it will also become an issue in the future (See Chaps. 5 and 7).
- An intrinsic loss of a material is caused by the relaxation of intrinsic defect states in the bulk or surface of the material. In general, intrinsic loss could not be measured directly because of the loss coming from the support for the measurement. To solve this problem, a nodal support system, which in principle does not introduce any external loss to the sample by supporting it at their nodal points, was proposed by Kenji Numata in 2000 [10]. Since then, this technique has been used [11, 12]. In our case, it was estimated using a torsional mode (See Chap. 6), similarly to that described in Ref. [13].

The various dissipation processes contribute independently to the overall mechanical losses, and hence add up incoherently. The resulting mechanical quality factor, Q_{total}, is given by $1/Q_{total} = \sum_i 1/Q_i$, where i labels the different loss mechanisms.

Since the loss of the energy is only associated with the elastic part of the stored energy, the mechanical dissipation can be mitigated by storing most of the mechanical energy in a nearly lossless gravitational or optical potential, thereby strongly diluting the effect of the dissipation.

- **Gravitational dilution:** The total mechanical loss of an oscillator is diluted with gravity by a factor of k_{grav}/k_{el}, where k_{grav} and k_{el} are the gravitational and elastic spring constants [14]. The mechanical quality factor thus becomes about k_{grav}/k_{el}-times larger. This effect can be given by using loss angle ϕ, as below

$$k_{\rm el}(1+i\phi)+k_{\rm g}=\left(1+\frac{k_{\rm g}}{k_{\rm el}}\right)k_{\rm el}\left[1+\frac{i\phi}{1+\frac{k_{\rm g}}{k_{\rm el}}}\right]\simeq k_{\rm g}\left[1+\frac{i\phi}{1+\frac{k_{\rm g}}{k_{\rm el}}}\right]. \quad (2.44)$$

The loss angle is given by using the quality factor, Q, as follows

$$Q=\frac{1}{\phi}\left(\text{structure damping, i.e., } \gamma=\frac{\omega_{\rm g}^2}{2Q\omega}\right), \text{ or} \quad (2.45)$$

$$=\frac{1}{\phi}\frac{\omega}{\omega_{\rm g}}\left(\text{viscous damping, i.e., } \gamma=\frac{\omega_{\rm g}}{2Q}\right). \quad (2.46)$$

Thus, the quality factor is enhanced by the gravitational dilution by a factor of $Q_{\rm en}$, which is given by

$$Q_{\rm en}=\left(1+\frac{k_{\rm g}}{k_{\rm el}}\right). \quad (2.47)$$

In practice, only $k_{\rm el}$ is variable, and thus thermal fluctuating force is also diluted as below,

$$S^{\prime(2)}_{\rm FF,th}=4k_{\rm B}T\frac{\omega_{\rm g}}{2Q'}\simeq S^{(2)}_{\rm FF,th}\frac{k_{\rm el}}{k_{\rm g}} \quad (2.48)$$

Here, $S^{(2)}_{\rm FF,th}$ is thermal noise with the small gravitational dilution, while the parameters with prime indicates the similar but with the large gravitational dilution. In our case, an ultimate thin wire (the radius is 1.5 μm) assures that the amount of energy stored in the pendulum is dominated by the gravitational potential over the elastic bending energy of the wire. More concretely, the mechanical dissipation is about 600-times diluted (See Chaps. 5 and 6).

- **Optical dilution:** Mechanical energy is stored in the lossless potential provided by the optical restoring forces, which dilutes the effects of internal material dissipation. The mechanical quality factor thus becomes about $k_{\rm opt}/k_{\rm el}$-times and $\omega_{\rm opt}/\omega_{\rm el}$-times larger for the structure damping case and the viscous damping case, respectively. Here, $f_{\rm eff}$ is the effective resonant frequency of the mechanical oscillator trapped by the optical spring. In the case of the *soft* suspension, such as the suspended mirror, this effect is relatively increased, and thereby it is often used with pendulums [15–17]. This effect can be given by using loss angle ϕ, as below

$$k_{\rm el}(1+i\phi)+k_{\rm opt}=\left(1+\frac{k_{\rm opt}}{k_{\rm el}}\right)k_{\rm el}\left[1+\frac{i\phi}{1+\frac{k_{\rm opt}}{k_{\rm el}}}\right]. \quad (2.49)$$

The loss angle is given by using the quality factor, Q, as follows

$$Q = \frac{1}{\phi}\left(\text{structure damping, i.e., } \gamma = \frac{\omega_{\rm el}^2}{2Q\omega}\right), \text{ or} \tag{2.50}$$

$$= \frac{1}{\phi}\frac{\omega}{\omega_{\rm el}}\left(\text{viscous damping, i.e., } \gamma = \frac{\omega_{\rm el}}{2Q}\right). \tag{2.51}$$

Thus, the quality factor is enhanced by the optical dilution by a factor of $Q_{\rm en}$, which is given by

$$Q_{\rm en} = \left(1 + \frac{k_{\rm opt}}{k_{\rm el}}\right)(\text{structure damping}), \text{ or} \tag{2.52}$$

$$\simeq \left(\frac{\omega_{\rm el}}{\omega_{\rm opt}} + \frac{\omega_{\rm opt}}{\omega_{\rm el}}\right) \simeq \frac{\omega_{\rm opt}}{\omega_{\rm el}}(\text{viscous damping}). \tag{2.53}$$

In practice, $k_{\rm opt}$ is variable, and thus thermal fluctuating force is *not* diluted as below,

$$S_{\rm FF,th}^{\prime(2)} = 4k_{\rm B}T\frac{\omega_{\rm opt}}{2Q'} = 4k_{\rm B}T\frac{\omega_{\rm el}}{2Q} = S_{\rm FF,th}^{(2)} \tag{2.54}$$

Here, $S_{\rm FF,th}^{(2)}$ is thermal noise with the small gravitational dilution, while the parameters with prime indicates the similar but with the large gravitational dilution. In our case, the effective frequency of the pendulum is enhanced from 2 to 400 Hz (See Chap. 6).

We note that the only gravitational dilution can reduce thermal fluctuating force from Eqs. (2.48) and (2.54), since we naturally suppose that the gravitational dilution is changed without changing the gravitational potential, while the optical dilution is changed by changing the optical potential. The dilution techniques mentioned above have a key to experimentally investigate the macroscopic quantum mechanics because any macroscopic object is strongly affected by thermal decoherence as just it is. When the oscillator is trapped and damped by the nearly lossless field, the Eq. (2.41) is given by

$$\frac{d}{dt}\langle n\rangle = -2\gamma_{\rm m}\left(\langle n\rangle - \bar{n}_{\rm th}\right) - 2\gamma_{\rm eff}\left(\langle n\rangle - \bar{n}_{\rm th,eff}\right), \tag{2.55}$$

where $\gamma_{\rm eff}$ is the effective mechanical decay rate, $\bar{n}_{\rm th,eff}$ (becomes zero for lossless fields) is the effective thermal occupation number of the effective bath, and here we also suppose the mechanical decay rate and effective decay rate have *no* dependence on frequency (i.e., viscous damping model is supposed). Here, the number of coherent oscillations in the presence of thermal decoherence is given by

$$n_{\mathrm{osc}} = \frac{\hbar}{2k_{\mathrm{B}}T_{\mathrm{th}}} \times \frac{\omega_{\mathrm{eff}}^2}{\gamma_{\mathrm{m}}}, \\ = Q_{\mathrm{m}} \cdot f_{\mathrm{m}} \times \frac{h}{k_{\mathrm{B}}T_{\mathrm{th}}} \times \left(\frac{\omega_{\mathrm{eff}}}{\omega_{\mathrm{m}}}\right)^2. \tag{2.56}$$

Thus, the requirement for room-temperature quantum optomechanics is mitigated by a factor of $(\omega_{\mathrm{eff}}/\omega_{\mathrm{m}})^2$. In our case, the original $Q_{\mathrm{m}} \cdot f_{\mathrm{m}}$ is about 1×10^6 Hz, which is about 6×10^6-times lower than the original requirement, even though the gravitational potential increases the mechanical quality factor. The optical spring further reduces the difference to $6 \times 10^6 \cdot (2/400)^2 = 150$ at the least. In practically, since our measurement determined the dissipation model as structure damping, the requirement ought to be further mitigated (but it is not calculated now). Also, the effective phonon number of the mechanical oscillator is given by

$$n_{\mathrm{eff}} = \frac{k_{\mathrm{B}}T_{\mathrm{th}}}{\hbar\omega_{\mathrm{m}}} \times \left(\frac{\omega_{\mathrm{m}}}{\omega_{\mathrm{eff}}}\right)^2 \times \frac{Q_{\mathrm{eff}}}{Q_{\mathrm{m}}}, \\ = \frac{Q_{\mathrm{eff}}}{n_{\mathrm{osc}}}. \tag{2.57}$$

Thus, if the requirement for $f \cdot Q$ product is satisfied, n_{eff} can be reduced under one with Q_{eff} over one.

2.3 Optomechanical System

2.3.1 Theoretical Derivation of Quantum Back-Action

Here, we calculate the quantum back-action in the optomechanical system shown in Fig. 2.4. We again start from Newton's law to describe the mechanical response,

$$m\ddot{x} + 2m\gamma_{\mathrm{m}}\dot{x} + k_{\mathrm{m}}x = F, \tag{2.58}$$

where m is the mass of the movable mirror (mechanical oscillator), ω_{m} is the mechanical resonant frequency, γ_{m} is the mechanical amplitude decay rate, k_{m} is the mechanical spring constant, and x is the position for the mirror. To derive the mechanical susceptibility, we Fourier transform Eq. (2.58) according to the following conventions: $f(\omega) \equiv \int_{-\infty}^{\infty} dt f(t) \exp(-i\omega t)$,

$$\chi_{\mathrm{m}} \equiv \frac{x}{F} = \frac{1}{m(\omega_{\mathrm{m}}^2 - \omega^2 + i2\omega\gamma_{\mathrm{m}})}. \tag{2.59}$$

Let us next calculate the response of an optomechanical system to two independent laser driving fields. We consider the two beams in order to explain so-called "double optical spring" [18]. The Hamiltonian describing the optomechanical coupling [19] can be written and linearized in the form

$$\begin{aligned}\hat{\mathscr{H}} &= \hbar\omega_{\mathrm{c}}(x)\hat{a}^{\dagger}\hat{a} + \hbar\omega_{\mathrm{c}}(x)\hat{b}^{\dagger}\hat{b} + \hat{\mathscr{H}}_{\kappa} \\ &\simeq \hbar\omega_{\mathrm{c}}\hat{a}^{\dagger}\hat{a} + \hbar\omega_{\mathrm{c}}\hat{b}^{\dagger}\hat{b} + \hbar g\hat{a}^{\dagger}\hat{a}x + \hbar g\hat{b}^{\dagger}\hat{b}x + \hat{\mathscr{H}}_{\kappa},\end{aligned} \tag{2.60}$$

where $g = 2\omega_{\mathrm{c}}\cos\beta/L$ is the optomechanical coupling constant[1] (the coupling constant will be given in Chap. 5, Sect. 5.2.4), ω_{c} is the cavity resonance frequency, β is the incident angle on the movable mirror, L is the round-trip length and $\hat{\mathscr{H}}_{\kappa}$ represents the optical input and output coupling; and $\hat{a}$ and $\hat{b}$ are the annihilation operators (cavity modes) for two counterpropagating directions in the triangular cavity, respectively. The Heisenberg Langevin equations of motion for the cavity modes are:

$$\dot{\hat{a}} = -(\kappa + i\omega_{\mathrm{c}})\hat{a} - ig_{\mathrm{a}}x\hat{a} + \sum_{\mathrm{l}}\sqrt{2\kappa_{\mathrm{l}}}\hat{A}_{\mathrm{l}}, \tag{2.61}$$

$$\dot{\hat{b}} = -(\kappa + i\omega_{\mathrm{c}})\hat{b} - ig_{\mathrm{b}}x\hat{b} + \sum_{\mathrm{l}}\sqrt{2\kappa_{\mathrm{l}}}\hat{B}_{\mathrm{l}}, \tag{2.62}$$

where the κ_{in1}, κ_{in2}, κ_{in3} are the cavity amplitude decay rates for each mirror, κ_{in4} is the decay rate for the cavity round-trip loss and κ is the total decay rate; $\hat{A}_{\mathrm{l}}$ and $\hat{B}_{\mathrm{l}}$ are the input optical fields. The equation of motion can be written in a rotating frame of reference by setting $\hat{a} = \exp(-i\omega_{\mathrm{a}}t)\hat{a}$ and linearized in the following form:

$$\dot{\delta\hat{a}} = -(\kappa - i\Delta_{\mathrm{a}})(\bar{\mathrm{a}} + \delta\hat{a}) - iG_{\mathrm{a}}\delta x + \sqrt{2\kappa_{\mathrm{in1}}}\bar{A}_{\mathrm{in1}} + \sum_{\mathrm{l}}\sqrt{2\kappa_{\mathrm{l}}}\delta\hat{A}_{\mathrm{l}}, \tag{2.63}$$

$$\dot{\delta\hat{b}} = -(\kappa - i\Delta_{\mathrm{b}})(\bar{b} + \delta\hat{b}) - iG_{\mathrm{b}}\delta x + \sqrt{2\kappa_{\mathrm{in2}}}\bar{B}_{\mathrm{in2}} + \sum_{\mathrm{l}}\sqrt{2\kappa_{\mathrm{l}}}\delta\hat{B}_{\mathrm{l}}, \tag{2.64}$$

where $\Delta_{\mathrm{a}} = \omega_{\mathrm{a}} - \omega_{\mathrm{c}} - G_{\mathrm{a}}\bar{x}$ and $\Delta_{\mathrm{b}} = \omega_{\mathrm{b}} - \omega_{\mathrm{c}} - G_{\mathrm{b}}\bar{x}$ are the cavity detuning; $G_{\mathrm{a}} = \bar{a}g$ and $G_{\mathrm{b}} = \bar{b}g$ are the light-enhanced optomechanical couplings for the linearized regime; $\bar{a}$ and $\bar{b}$ are the average parts for each cavity mode; $\delta\hat{a}$ and $\delta\hat{b}$ are the fluctuating parts for each cavity mode; $\bar{A}_{\mathrm{in1}}$ and $\bar{B}_{\mathrm{in2}}$ are the real valued coherent amplitudes for input lasers; $\delta\hat{A}_{\mathrm{l}}$ and $\delta\hat{B}_{\mathrm{l}}$, for $\mathrm{l} = \mathrm{in1}, \mathrm{in2}, \mathrm{in3}, \mathrm{in4}$ are the vacuum fluctuation entering from each port.

The average intracavity field amplitudes are described by Eqs. (2.63) and (2.64):

$$\bar{a} = \frac{\sqrt{2\kappa_{\mathrm{in1}}}}{\kappa - i\Delta_{\mathrm{a}}}\bar{A}_{\mathrm{in1}}, \tag{2.65}$$

[1] optomechanical single-photon coupling strength g_0 (e.g. in Ref. [8, 20]), which gives $\hat{\mathscr{H}} = \hbar g_0\hat{a}^{\dagger}\hat{a}(\hat{b} + \hat{b}^{\dagger})$, is x_{zpf}-times lager than g.

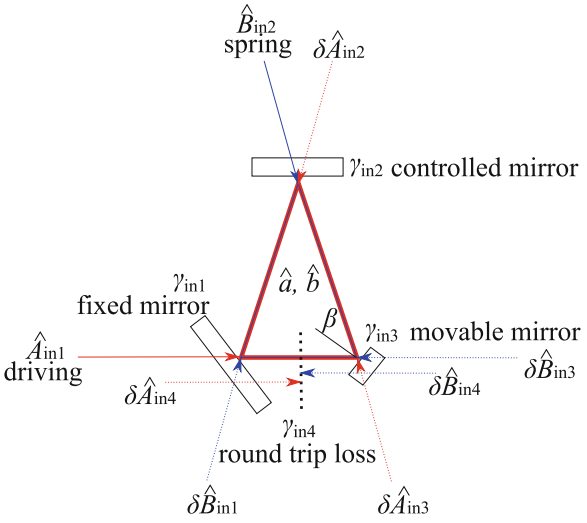

Fig. 2.4 Layout of the triangular cavity. The cavity consists of three mirrors: the input coupler for the driving beam, with a decay rate of κ_{in1}; the input coupler for the spring beam, with a decay rate of κ_{in2}; the movable mirror, with a decay rate of κ_{in3}; and a mirror to represent intracavity loss, with a decay rate of κ_{in4}. The cavity mode is labeled $\hat{a}$ and $\hat{b}$. The extracavity fields are: $\hat{A}_{in1}$, $\delta\hat{A}_{in2}$, $\delta\hat{A}_{in3}$, $\delta\hat{A}_{in4}$, $\delta\hat{B}_{in1}$, $\hat{B}_{in2}$, $\delta\hat{B}_{in3}$, and $\delta\hat{B}_{in4}$

$$\bar{b} = \frac{\sqrt{2\kappa_{in2}}}{\kappa - i\Delta_b}\bar{B}_{in2}. \tag{2.66}$$

From these equations, the intracavity power is given by

$$\begin{aligned}\bar{P}_{circ} &= \frac{\hbar\omega_c|a|^2}{\tau} + \frac{\hbar\omega_c|b|^2}{\tau} \\ &= \frac{2\kappa_{in1}}{\tau(\kappa^2+\Delta_a^2)}\bar{P}_{in1} + \frac{2\kappa_{in2}}{\tau(\kappa^2+\Delta_b^2)}\bar{P}_{in2}, \\ &= \bar{P}_{in1,circ} + \bar{P}_{in2,circ}\end{aligned} \tag{2.67}$$

where τ is the cavity round-trip time.

The fluctuation components of Eqs. (2.63) and (2.64) are similarly at given by

$$\dot{\delta\hat{a}} = -(\kappa - i\Delta_a)\delta\hat{a} - iG_a\delta x + \sum_l \sqrt{2\kappa_l}\delta\hat{A}_l, \tag{2.68}$$

$$\dot{\delta\hat{b}} = -(\kappa - i\Delta_b)\delta\hat{b} - iG_b\delta x + \sum_l \sqrt{2\kappa_l}\delta\hat{B}_l. \tag{2.69}$$

In terms of the frequency components, these can be rewritten by

$$\delta\hat{a} = \chi_a(-iG_a\delta x + \sum_l \sqrt{2\kappa_l}\delta\hat{A}_l), \tag{2.70}$$

$$\delta\hat{b} = \chi_b(-iG_b\delta x + \sum_l \sqrt{2\kappa_l}\delta\hat{B}_l). \tag{2.71}$$

Here, $\chi_a = (\kappa + i(\omega - \Delta_a))^{-1}$ and $\chi_b = (\kappa + i(\omega - \Delta_b))^{-1}$ are the cavity susceptibilities for the two modes. These lead to forces induced by the cavity modes, being applied to the movable mirror, which are given by:

$$\bar{F}_{BA} = -\frac{(g_a + g_b)\tau}{\omega_c}\bar{P}_{circ}, \tag{2.72}$$

$$\delta F_{BA} = i\hbar|G_a|^2\delta x(\chi_a(\omega) - \chi_a^*(-\omega)) + i\hbar|G_b|^2\delta x(\chi_b(\omega) - \chi_b^*(-\omega)), \tag{2.73}$$

$$\begin{aligned}\delta\hat{F}_{BA} = &-\hbar G_a^*\chi_a(\omega)\sum_l \sqrt{2\kappa_l}\delta\hat{A}_l - \hbar G_a\chi_a^*(-\omega)\sum_l \sqrt{2\kappa_l}\delta\hat{A}_l^\dagger \\ &- \hbar G_b^*\chi_b(\omega)\sum_l \sqrt{2\kappa_l}\delta\hat{B}_l - \hbar G_b\chi_b^*(-\omega)\sum_l \sqrt{2\kappa_l}\delta\hat{B}_l^\dagger,\end{aligned} \tag{2.74}$$

where $\bar{F}_{BA}$ is the average back-action force, δF_{BA} is the dynamic back-action, which influences the dynamics of the harmonically bound mirror, and $\delta\hat{F}_{BA}$ is the quantum back-action force.

From the dynamic back-action, the optical spring effect is given by

$$\begin{aligned}K(\omega) = -\frac{\delta F_{BA}}{\delta x} &= 2\hbar|G_a|^2\frac{\Delta_a}{(\kappa + i\omega)^2 + \Delta_a^2} + 2\hbar|G_b|^2\frac{\Delta_b}{(\kappa + i\omega)^2 + \Delta_b^2} \\ &= \frac{8P_{in1,circ}\omega_c}{Lc}\frac{\Delta_a\cos^2(\beta)}{(\kappa + i\omega)^2 + \Delta_a^2} + \frac{8P_{in2,circ}\omega_c}{Lc}\frac{\Delta_b\cos^2(\beta)}{(\kappa + i\omega)^2 + \Delta_b^2}.\end{aligned} \tag{2.75}$$

The experiment is performed under the "slowly varying" condition, $\omega \ll \sqrt{\Delta_a^2 + \kappa^2}$; then, the spring effect can be written by

$$\begin{aligned}K &= 2\hbar|G_a|^2\left[\frac{\Delta_a}{\kappa^2 + \Delta_a^2} - \frac{2i\kappa\Delta_a}{(\kappa^2 + \Delta_a^2)^2}\omega\right] + 2\hbar|G_b|^2\left[\frac{\Delta_b}{\kappa^2 + \Delta_b^2} - \frac{2i\kappa\Delta_b}{(\kappa^2 + \Delta_b^2)^2}\omega\right] \\ &\equiv K_{opt} + i\omega\Gamma_{opt}.\end{aligned} \tag{2.76}$$

This condition is also called the "bad" cavity condition because of the weakness of the cooling effect due to the delay of light itself. Under this condition, the intracavity optical power is largely increased as an effect of the laser cooling being increased, and thereby the back-action is also increased. If the light-enhanced optomechanical coupling constant, G, is larger than $\sqrt{m\kappa\gamma_m\omega_m}/\hbar$, the back-action becomes larger than the SQL on resonance of the mechanical oscillator. Thus, in general, this condition is not appropriate for the laser (passive) cooling of the object for achieving its ground state (this condition is suitable for feed-back cooling [21]). On the other hand, in the resolved sideband regime, defined as $\omega_m \gg \kappa$, one can reduce the occupation number to $(\kappa/2\omega_m)^2$ [22, 23]. Therefore, this condition is called the "good" cavity condition.

This spring modifies the dynamics of the mirror as

$$\omega_{\rm eff}^2 = \omega_{\rm m}^2 + \frac{K_{\rm opt}}{m}, \tag{2.77}$$

$$\gamma_{\rm eff} = \gamma_{\rm m} + \frac{\Gamma_{\rm opt}}{2m}, \tag{2.78}$$

which indicates that the positive (negative) rigidity is always accompanied by negative (positive) damping. In either case, the system is unstable if we use a single optical spring. To stabilize the system, one can use a feedback control; however, it is difficult to control if we use a tiny oscillator. An appropriate alternative is to implement the idea of the double optical spring [18], by inputting two lasers to the cavity at different frequencies. One laser with a small detuning provides a large positive damping, while the other higher input-power beam with a large detuning provides a strong restoring force. The resulting system is self-stabilized with both positive rigidity and positive damping, as shown in Fig. 2.5. In addition, unlike mechanical springs, the optical spring effect does not change the thermal excitation spectrum of the mirror, since the optical field is almost in its ground state (in our case, the infrared optical field has an effective temperature of 15,000 K). We can measure the quantum back-action force fluctuation as a displacement fluctuation via the effective susceptibility, $\chi_{\rm eff}$.

The double-sided force spectrum, $S_{FF,q}^{(2)}$, is written as

$$\begin{aligned} S_{\rm FF,q}^{(2)} &= \langle \delta \hat{F}_{\rm BA}(-\omega) \delta \hat{F}_{\rm BA}(\omega) \rangle \\ &= 2\hbar^2 \kappa |G_{\rm a}|^2 |\chi_{\rm a}(-\omega)|^2 + 2\hbar^2 \kappa |G_{\rm b}|^2 |\chi_{\rm b}(-\omega)|^2 \\ &= 2N_{\rm in1,circ} \frac{\hbar^2 g^2}{\kappa} \left(1 + \left(\frac{\omega + \Delta_{\rm a}}{\kappa} \right)^2 \right)^{-1} + 2N_{\rm in2,circ} \frac{\hbar^2 g^2}{\kappa} \left(1 + \left(\frac{\omega + \Delta_{\rm b}}{\kappa} \right)^2 \right)^{-1}. \end{aligned} \tag{2.79}$$

Therefore, the quantum back-action is given by $|\chi_{\rm eff}|^2 S_{\rm FF,q}^{(2)}$ as displacement fluctuations (in the unit of m^2/Hz). The ratio of the quantum back-action to thermal fluctuating force is then given by

$$\frac{S_{\rm FF,q}^{(2)}}{S_{\rm FF,th}^{(2)}} = \frac{1}{n_{\rm th}} \frac{N_{\rm circ} g^2}{\kappa \gamma_{\rm m}}. \tag{2.80}$$

Here, $N_{\rm circ}$ is the intracavity photon number of the single laser, which dominates the quantum back-action, and we suppose the bad cavity condition.

In practice, a laser has a classical intensity fluctuation generating the "classical" back-action force. This effect is given by

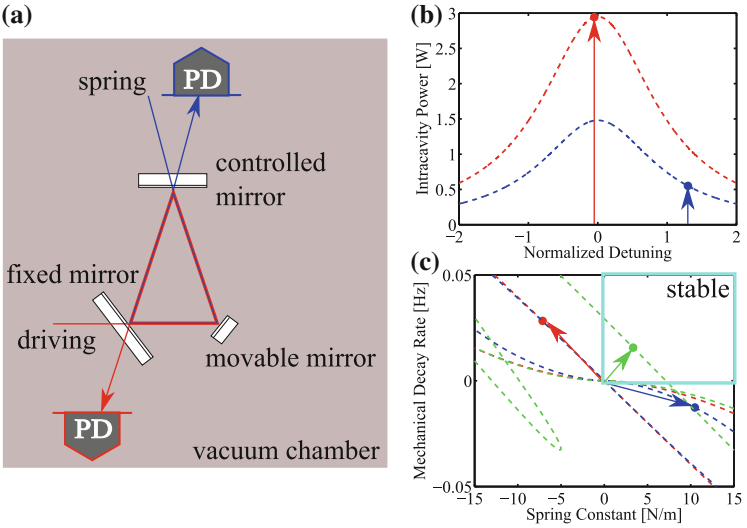

Fig. 2.5 The double optical spring effect. a The beams illustrated as the *red* and the *blue lines* incident on the fixed and controlled mirrors, respectively. **b** The intracavity power and detuning for each beam. The *red* and *blue* points show both laser-cavity detuning and the intracavity power. The *dashed red* and *blue curves* show the optical power as a function of the cavity detuning for each beam. The driving beam dominates the quantum back-action due to the higher intracavity power than the spring beam. **c** The optical spring effect. The *red* point represents the beam illustrated as the *red line* at $\Delta_a/\kappa = -0.05$, the *blue* point represents the beam illustrated as the *blue line* at $\Delta_b/\kappa = +1.3$, and the *dashed green* represents their sum. The *dashed red* and *blue curves* show parametric plots of the optical spring as a function of the detuning for each beam, and the *dashed green curve* is their sum. Inside the cyan flame, both the spring and the mechanical decay rates have a positive values, and thus the mirror is stably trapped

$$S^{(2)}_{\mathrm{FF,c}} = 2(B_{\mathrm{in1}} - 1)\hbar^2\kappa_{\mathrm{in1}}|G_a|^2\left(|\chi_a(\omega) + \chi_a(-\omega)|^2\right) + 2(B_{\mathrm{in2}} - 1)\hbar^2\kappa_{\mathrm{in2}}|G_b|^2\left(|\chi_b(\omega) + \chi_b(-\omega)|^2\right), \tag{2.81}$$

where B_{in1} and B_{in2} are the relative shot noise levels for each beam.

2.3.2 Phase-Induced Radiation Pressure

Here, we present phase-induced radiation pressure noise [24]. Phase fluctuations of the laser induce force fluctuations imposed on the mirror similar to that of intensity fluctuations, if the cavity is *detuned* from the resonance. The detuned cavity generates phase difference between the input laser and the intracavity field, and thus phase fluctuations of the input laser contributes to intensity fluctuations inside the cavity. To present a detailed expression of the phase-induced radiation pressure, we consider an intracavity field $a(t)$, which is input to the small phase-modulated beam

($d\varphi \ll 1$). The intracavity field is expanded to the first order of the Bessel-functions as below [25]

$$a(t) \propto \frac{1}{\kappa + i\Delta} + \frac{e^{i\Omega_{\mathrm{m}}t}/2}{\kappa + i(\Delta + \Omega_{\mathrm{m}})}d\varphi - \frac{e^{-i\Omega_{\mathrm{m}}t}/2}{\kappa + i(\Delta - \Omega_{\mathrm{m}})}d\varphi, \tag{2.82}$$

where Ω_{m} is a modulation frequency, and $d\varphi$ is the phase fluctuations. We respectively define e^{+} and e^{-} as $e^{i\Omega_{\mathrm{m}}t}$ and $e^{-i\Omega_{\mathrm{m}}t}$ for simplicity, and then the intracavity intensity is calculated as below,

$$\begin{aligned}
|a(t)|^2 &\propto \left[\frac{1}{\kappa + i\Delta} + \frac{e^{+}/2}{\kappa + i(\Delta + \Omega_{\mathrm{m}})}d\varphi - \frac{e^{-}/2}{\kappa + i(\Delta - \Omega_{\mathrm{m}})}d\varphi\right] \\
&\times \left[\frac{1}{\kappa - i\Delta} + \frac{e^{-}/2}{\kappa - i(\Delta + \Omega_{\mathrm{m}})}d\varphi - \frac{e^{+}/2}{\kappa - i(\Delta - \Omega_{\mathrm{m}})}d\varphi\right], \\
&\simeq \frac{1}{\kappa^2 + \Delta^2} \\
&+ \frac{[\kappa - i(\Delta - \Omega_{\mathrm{m}})]e^{-}/2 - [\kappa - i(\Delta + \Omega_{\mathrm{m}})]e^{+}/2}{[\kappa - i(\Delta + \Omega_{\mathrm{m}})][\kappa - i(\Delta - \Omega_{\mathrm{m}})]}\frac{d\varphi}{\kappa + i\Delta} \\
&+ \frac{[\kappa + i(\Delta - \Omega_{\mathrm{m}})]e^{+}/2 - [\kappa + i(\Delta + \Omega_{\mathrm{m}})]e^{-}/2}{[\kappa + i(\Delta + \Omega_{\mathrm{m}})][\kappa + i(\Delta - \Omega_{\mathrm{m}})]}\frac{d\varphi}{\kappa - i\Delta}, \\
&\simeq \frac{1}{\kappa^2 + \Delta^2} \\
&+ \frac{-i(\kappa - i\Delta)\sin\Omega_{\mathrm{m}}t + i\Omega_{\mathrm{m}}\cos\Omega_{\mathrm{m}}t}{(\kappa - i\Delta)^2}\frac{d\varphi}{\kappa + i\Delta} \\
&+ \frac{i(\kappa + i\Delta)\sin\Omega_{\mathrm{m}}t - i\Omega_{\mathrm{m}}\cos\Omega_{\mathrm{m}}t}{(\kappa + i\Delta)^2}\frac{d\varphi}{\kappa - i\Delta}, \\
&= \frac{1}{\kappa^2 + \Delta^2} \\
&+ \frac{[-(i\kappa + \Delta)\sin\Omega_{\mathrm{m}}t + i\Omega_{\mathrm{m}}\cos\Omega_{\mathrm{m}}t](\kappa + i\Delta)}{(\kappa^2 + \Delta^2)^2}d\varphi \\
&+ \frac{[(i\kappa - \Delta)\sin\Omega_{\mathrm{m}}t - i\Omega_{\mathrm{m}}\cos\Omega_{\mathrm{m}}t](\kappa - i\Delta)}{(\kappa^2 + \Delta^2)^2}d\varphi, \\
&= \frac{1}{\kappa^2 + \Delta^2} \\
&+ \frac{-2\kappa\Delta\sin\Omega_{\mathrm{m}}t + 2i\Delta(-i\kappa\sin\Omega_{\mathrm{m}}t + i\Omega_{\mathrm{m}}\cos\Omega_{\mathrm{m}}t)}{(\kappa^2 + \Delta^2)^2}d\varphi, \\
&= \frac{1}{\kappa^2 + \Delta^2} - \frac{2\Delta\Omega_{\mathrm{m}}\cos\Omega_{\mathrm{m}}t}{(\kappa^2 + \Delta^2)^2}d\varphi,
\end{aligned} \tag{2.83}$$

where, we suppose the condition of $\kappa \gg \Omega_{\mathrm{m}}$. Thus, the radio of radiation pressure fluctuations (zeroth-order term) to phase-induced radiation pressure fluctuations (first-order term) is given by,

$$\frac{S_{\text{phase}}}{S_{\text{rad}}} = -\frac{2\Delta\Omega_{\text{m}}\cos\Omega_{\text{m}}t}{\kappa^2+\Delta^2}d\varphi, \\ = -\frac{2\Omega_{\text{m}}\cos\Omega_{\text{m}}t}{\kappa}\frac{\delta}{1+\delta^2}d\varphi, \tag{2.84}$$

where $\delta \equiv \Delta/\kappa$ is the normalized detuning. From this equation, phase-induced radiation pressure noise is negligible small if the bad cavity condition is valid. In our measurements shown in Chap. 6, roughly only 0.3 % of the force fluctuation is due to the phase noise.

2.3.3 Photo-Thermal Shot Noise

Here, we present photo-thermal shot noise [26, 27], which is caused by optical power fluctuations absorbed in dielectrical reflective layers. The fluctuated power absorption makes the fluctuation of the mirror's surface through the thermal expansion coefficient. The photo-thermal shot noise $S^{(2)}_{\text{FF,photo-thermal}}$ is given by

$$S^{(2)}_{\text{FF,photo-thermal}} = \frac{2\alpha^2(1+\sigma)^2\hbar\omega_{\text{c}}T_{\text{abs}}P_{\text{circ}}m\omega^2}{(\rho C\pi r_0^2)^2}. \tag{2.85}$$

Here, α is thermal expansion coefficient, σ is the Poisson coefficient, T_{abs} is the absorption coefficient of the 5-mg mirror, P_{circ} is intra-cavity power, ρ is density of the mirror, C is specific heat capacity of the mirror, r_0 is the spot size on the mirror. In our measurements, it is maximumly only 0.2 % of the quantum back-action.

2.3.4 Raman Decoherence

Here, we present Raman decoherence [28], which is induced by Raman scattering of the optical pump field. To make the point clarify, the effect of the optical spring given by Eq. (2.75) is divided into following two terms as,

$$\frac{1}{(\kappa+i\omega)^2+\Delta^2} = \frac{\kappa^2+\Delta^2-\omega^2-2i\kappa\omega}{(\kappa^2+(\Delta-\omega)^2)(\kappa^2+(\Delta+\omega)^2)} \\ = \frac{\kappa^2+\Delta^2-\omega^2-2i\kappa\omega}{4\Delta\omega}\left[\frac{1}{(\kappa^2+(\Delta-\omega)^2)}-\frac{1}{(\kappa^2+(\Delta+\omega)^2)}\right]. \tag{2.86}$$

Thus, the optical damping effect (imaginary part of the optical spring) is given by

$$\gamma_{\text{opt}} = A_+ - A_- \tag{2.87}$$

$$A_{\pm} = \frac{\hbar\kappa|G|^2}{2m\omega(\kappa^2 + (\Delta \pm \omega)^2)}. \tag{2.88}$$

This equation is interpreted as the difference between anti-Stokes (A_+) and Stokes (A_-) scattering rates, because $A_{\pm}$ define the rates at which laser photons are scattered by the moving oscillator simultaneously with the absorption or emission of the oscillator vibrational phonons [21]. Note that the Raman scattering destroy quantum coherence of the carrier light, which is given by the sum of the anti-Stokes and Stokes scattering rates, although two Raman scattering events has no net effect in terms of energy. Now, let us focus on only the beam that leads to stiffening in relevant regime of large detuning $\Delta \gg \omega$, in order to obtain the effective quality factor under the Raman decoherence. This is given by

$$Q_{\mathrm{Raman}} \equiv \frac{\omega_{\mathrm{eff}}}{2\gamma_{\mathrm{Raman}}} \simeq \frac{\Delta}{\kappa}\frac{\omega}{g}\sqrt{\frac{m\omega_{\mathrm{c}}\Delta^3}{\kappa P_{\mathrm{in}}}} \simeq \frac{\Delta}{\kappa}, \tag{2.89}$$

where γ_{Raman} is defined as $A_+ + A_-$. From this equation, one can find that the large input power and the large detuning are necessary in order to increase the resonant frequency of the mechanical oscillator, with reducing the Raman decoherece at the same time.

References

1. Heisenberg, W.: Über den anschaulichen Inhalt der quantentheoretischen Kinematik und Mechanik. Z. Phys. **43**, 172–198 (1927)
2. Rüdiger, A., et al.: A mode selector to suppress fluctuations in laser beam geometry. Optica Acta **28**, 641 (1981)
3. Walls, D.F., Milburn, G.J.: Quantum Optics. Springer, New York (1994)
4. White, A.G.: Classical and quantum dynamics of optical frequency conversion. Ph.D. thesis, Physics Department, The Australian National University, Canberra, Australia (1995)
5. McKenzie, K.: Squeezing in the audio gravitational wave detection band, Ph.D. thesis, Physics Department, The Australian National University, Canberra, Australia (2008)
6. Callen, H.B., Welton, T.A.: Irreversibility and generalized noise. Phys. Rev. **83**, 34 (1951)
7. Gonzalez, G.I., Saulson, P.R.: Brownian motion of a mass suspended by an anelastic wire. J. Acoust. Soc. Am. **96**, 1 (1994)
8. Aspelmeyer, M., Kippenberg, T.J., Marquardt, F.: Cavity optomechanics. Rev. Mod. Phys. **86**, 1391 (2014)
9. Saulson, P.R.: Fundamentals of Interferometric Gravitational Wave Detectors. World Scientific, Singapore (1994)
10. Numata, K., et al.: Measurement of the intrinsic mechanical loss of low-loss samples using a nodal support. Phys. Rev. A. **276**, 37 (2000)
11. Numata, K., et al.: Measurement of the mechanical loss of crystalline samples using a nodal support. Phys. Rev. A. **284**, 162 (2001)
12. Cole, G.D., Wilson-Rae, I., Werbach, K., Vanner, M.R., Aspelmeyer, M.: Phonon-tunnelling dissipation in mechanical resonators. Nat. Commun. **2**, 231 (2011)
13. Gonzalez, G., Saulson, P.R.: Brownian motion of a torsion pendulum with internal friction. Phys. Rev. A. **201**, 1 (1995)

14. Saulson, P.R.: Thermal noise in mechanical experiments. Phys. Rev. D. **42**, 8 (1990)
15. Corbitt, T., et al.: Optical dilution and feedback cooling of a Gram-Scale Oscillator to 6.9 mK. Phys. Rev. Lett. **99**, 160801 (2007)
16. Chang, D.E., Ni, K.-K., Painter, O., Kimble, H.J.: Ultrahigh-Q mechanical oscillators through optical trapping. New J. of Phys. **14**, 045002 (2012)
17. Ni, K.-K., et al.: Enhancement of mechanical Q factors by optical trapping. Phys. Rev. Lett. **108**, 214302 (2012)
18. Corbitt, T., et al.: An all-optical trap for a gram-scale mirror. Phys. Rev. Lett. **98**, 150802 (2007)
19. Law, C.K.: Interaction between a moving mirror and radiation pressure: a Hamiltonian formulation. Phys. Rev. A. **51**, 3 (1995)
20. Purdy, T.P., Peterson, R.W., Regal, C.A.: Observation of radiation pressure shot noise on a macroscopic object. Science **339**, 801 (2013)
21. Genes, C., Vitali, D., Gigan, S., Aspelmeyer, M.: Ground-state cooling of a micromechanical oscillator: comparing cold damping and cavity-assisted cooling schemes. Phys. Rev. A. **77**, 033804 (2008)
22. Wilson-Rae, L., Nooshi, N., Zwerger, W., Kippenberg, T.J.: Theory of ground state cooling of a mechanical Oscillator using dynamical back-action. Phys. Rev. Lett. **99**, 093901 (2007)
23. Marquardt, F., Chen, J.P., Clerk, A.A., Girvin, S.M.: Quantum theory of cavity-assisted sideband cooling of mechanical motion. Phys. Rev. Lett. **99**, 093902 (2007)
24. Rabl, P., Genes, C., Hammerer, K., Aspelmeyer, M.: Phase-noise induced limitations on cooling and coherent evolution in optomechanical systems. Phys. Rev. A. **80**, 063819 (2009)
25. Schliesser, A., Rivière, R., Anetsberger, G., Arcizet, O., Kippenberg, T.J.: Resolved sideband cooling of a micromechanical Oscillator. Nat. Phys. **4**, 415–419 (2008)
26. Braginsky, V.B., Gorodetsky, M.L., Vyatchanin, S.P.: Thermodynamical fluctuations and photo-thermal shot noise in gravitational wave antennae. Phys. Lett. A **264**, 1–10 (1999)
27. Restrepo, J., Gabelli, J., Ciuti, C., Favero, I.: Classical and quantum theory of photothermal cavity cooling of a mechanical oscillator. Comptes Rendus Physique **12**, 860–870 (2011)
28. Chang, C.E., Ni, K.-K., Painter, O., Kimble, H.J.: Ultrahigh-Qmechanical oscillators through optical trapping. New J. Phys. **14**, 045002 (2012)

http://www.springer.com/978-4-431-55880-4

Classical Pendulum Feels Quantum Back-Action

Matsumoto, N.

2016, XII, 103 p. 36 illus., 5 illus. in color., Hardcover
ISBN: 978-4-431-55880-4